NANO LETTERS

pubs.acs.org/NanoLett
Letter

Silver Electrodeposition from Ag/AgCl Electrodes: Implications for Nanoscience

Chuhongxu Chen,* Ziwei Wang, Guilin Chen, Zhijia Zhang, Zakhar Bedran, Stephen Tipper, Pablo Diaz-Núñez, Ivan Timokhin, Artem Mishchenko,* and Qian Yang*

Cite This: *Nano Lett.* 2025, 25, 9427−9432
Read Online

ABSTRACT: With the advancement of nanoscience, silver/silver chloride (Ag/AgCl) electrodes have become widely utilized in microscale and nanoscale fluidic experiments, because of their stability. However, our findings reveal that the dissolution of AgCl from the electrode in Cl^--rich solutions can lead to significant silver contamination, through the formation of silver complexes, $[AgCl_{n+1}]^{n-}$. We demonstrate the electrodeposition of silver particles on graphene in KCl aqueous solution, with AgCl dissolution from the electrode as the sole source of silver. This unexpected electrodeposition process offers a more plausible interpretation of the recently reported "ionic flow-induced current in graphene." That is, the measured electronic current in graphene is due to the electrodeposition of silver, challenging the previously claimed "ionic Coulomb drag". More caution is called for when using Ag/AgCl electrodes in microfluidic, and especially nanofluidic, systems because AgCl dissolution should not be neglected.

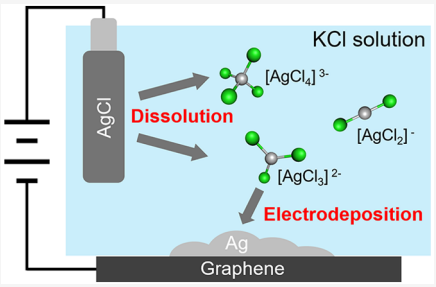

KEYWORDS: *Ag/AgCl electrode, electrodeposition, graphene, ionic Coulomb drag, nanofluidics*

The Ag/AgCl electrode is one of the most reliable reference electrodes used in electrochemistry, known for its stable electrode potential, low polarization, and reversible redox reactions.[1] In recent years, the Ag/AgCl electrode has repeatedly demonstrated its versatility in the advancing fields of two-dimensional (2D) membranes, biosequencing, nanofluidics, and their intersections. The research highlights encompass graphene,[2−4] nanopores,[5−11] nanochannels,[12,13] biosensors,[14−17] and ionic Coulomb drag.[18,19] The Ag/AgCl electrode is considered optimal in these cases because of its local solid-to-solid electrode reactions and low solubility product constant (K_{sp}),[20] and the contamination introduced to the experimental system was believed to be minimal. Therefore, the dissolution of AgCl in these systems, particularly involving Cl^- ions, has been overlooked so far in most studies. Using an electrochemical cell consisting of Ag/AgCl and monolayer graphene electrodes in the KCl aqueous solution, we report the direct observation of silver electrodeposition on graphene. As the sole source of silver in this system, the Ag/AgCl electrode induced significant and unexpected silver contamination. The electrodeposition of silver becomes even more important during our investigation of the "ionic Coulomb drag" phenomenon, where the electronic current in graphene is induced as a result of the silver electrodeposition, rather than the purported Coulomb interactions. Our findings serve as a reminder for future studies involving small-volume, ion-sensitive systems with exposed Ag/AgCl electrodes, as unintentional silver contamination could interfere with the intended experiments.

Using a two-electrode electrochemical cell (Figure 1a), we demonstrate the electrodeposition of silver on monolayer graphene, characterized by optical microscopy, energy-dispersive X-ray spectroscopy (EDX), and Raman spectroscopy. Figure 1b shows the graphene device, shaped in a Hall bar geometry similar to a typical GrFET sensor commonly used in other studies. A lab-made Ag/AgCl electrode (see Methods) was used to electrodeposit silver in a 1 M KCl solution with a constant bias voltage of 200 mV for 4 h. During the process, the gold contacts were exposed to the aqueous solution, with graphene connected to the circuit via the gold contact on the left. Figure 1b shows the optical micrograph of the same device made of chemical vapor deposited (CVD) graphene before and after electrodeposition (see also Figure S5a and b, the optical images of a mechanically exfoliated graphene device before and after silver electrodeposition). Black particles are seen on both graphene and gold contacts in the latter, showing significant deposition. Figure 1c shows the scanning electron microscopy (SEM) image of the region marked by the red square of Figure 1b. EDX analysis, shown in Figure 1d (mapping see supplementary Figure S1), demonstrates profound Ag peaks,

Received: March 29, 2025
Revised: May 6, 2025
Accepted: May 7, 2025
Published: May 28, 2025

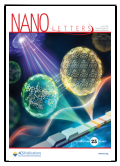

https://doi.org/10.1021/acs.nanolett.5c01929
Nano Lett. 2025, 25, 9427−9432

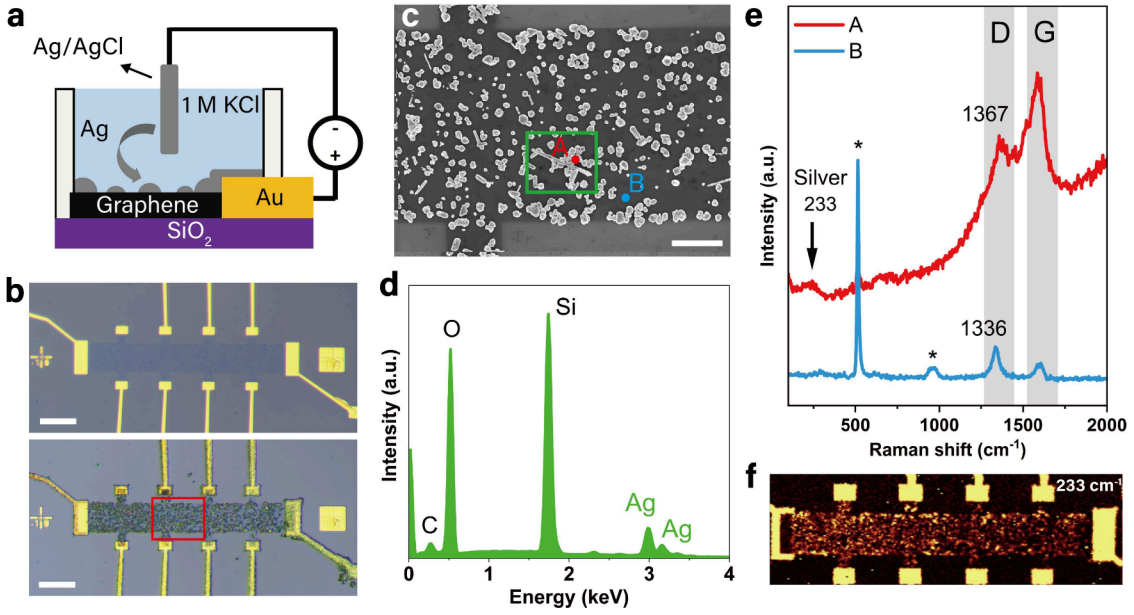

Figure 1. Characterization of the device after electrodeposition. (a) Schematic of the electrodeposition setup. An exposed Ag/AgCl electrode works as the counter electrode, and a monolayer CVD graphene flake works as the working electrode. (b) Optical images of the graphene device before (top) and after (bottom) the electrodeposition. Gold contacts were exposed to the solution during the experiment. Scale bar 25 μm. (c) SEM image of the area marked by the red square in (b). Scale bar 5 μm. (d) EDX spectrum collected in the area marked by the green square in (c). (e) Raman spectra of graphene with silver particles (A) and pristine graphene (B), collected on the spots marked by A and B in (c). The peaks marked by the asterisk are from SiO_2/Si substrate. (f) Raman intensity map of the peak at 233 cm^{-1} which shows the distribution of silver across the sample.

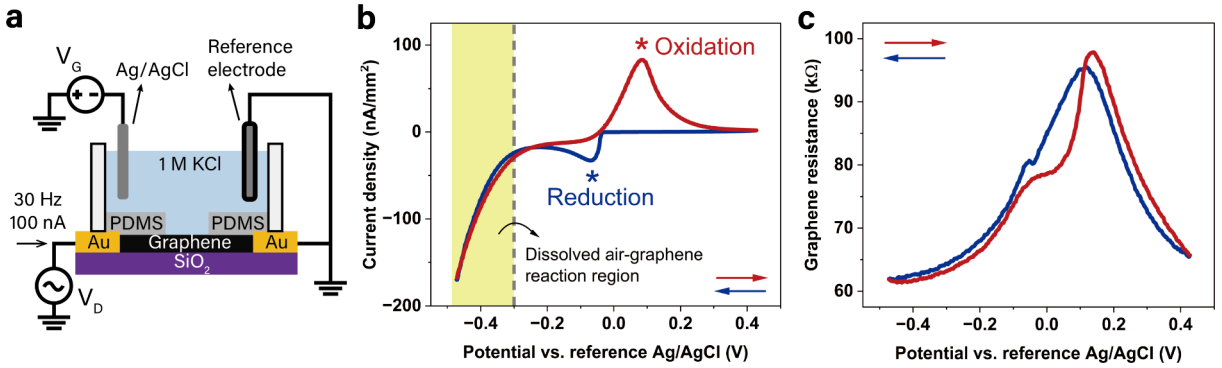

Figure 2. Electrodeposition process using a three-electrode electrochemical cell. (a) Schematic of the experimental setup for gating graphene and performing cyclic voltammetry. The setup consists of an Ag/AgCl counter electrode, a reference electrode and a graphene working electrode, forming a three-electrode electrochemical cell. Graphene resistance is monitored by applying a drain current of 100 nA at 30 Hz. V_G is the gate voltage, and V_D is the drain voltage. (b) Cyclic voltammogram and (c) graphene gating effect plotted against the gate potential (graphene potential vs reference electrode). Red and blue arrows indicate the direction of the potential sweep. Asterisks in (b) mark the oxidation and reduction peaks. The shaded yellow region highlights the reduction reaction of dissolved air in the solution at the graphene surface.

confirming that the deposited particles contain silver. Silver is known to be thermodynamically unstable and readily oxidizes under ambient conditions. For silver nanoparticles, this oxidation occurs even more rapidly.[21] Therefore, the deposited particles during the measurement are highly likely to have already undergone oxidation, forming a mixture of silver compounds. Additionally, to rule out potential defects in our lab-made electrodes, commercially available Ag/AgCl electrodes were also used in later experiments, and a similar electrodeposition was observed, see Figure S4.

We also conducted Raman spectroscopy to characterize the silver-deposited graphene. Figure 1e shows the Raman spectra collected over two positions on the device, A and B, with and without silver particles, as marked in Figure 1c. The silver particle greatly amplifies the Raman signal of graphene, causing a more significant background, stronger G and D bands, and a slight shift in the D band from 1336 cm^{-1} to 1367 cm^{-1}. This amplification can be explained by the localized surface plasmon resonance (LSPR) of metal particles, which is also the fundamental working principle of the surface enhanced Raman scattering (SERS) technique.[22] To map the landscape of deposited silver, we highlight a band at 233 cm^{-1}, which has been observed in many silver compounds.[23−28] Although studies usually associate this band with the Ag−Cl[25,26,28] or Ag−O[26,27] vibration, our observation aligns more with the Ag^0 plasmonic resonance,[23] with more details shown in the Supporting Information. Figure 1f presents an integrated intensity map of the Raman band centered at 233 cm^{-1} to

https://doi.org/10.1021/acs.nanolett.5c01929
Nano Lett. 2025, 25, 9427−9432

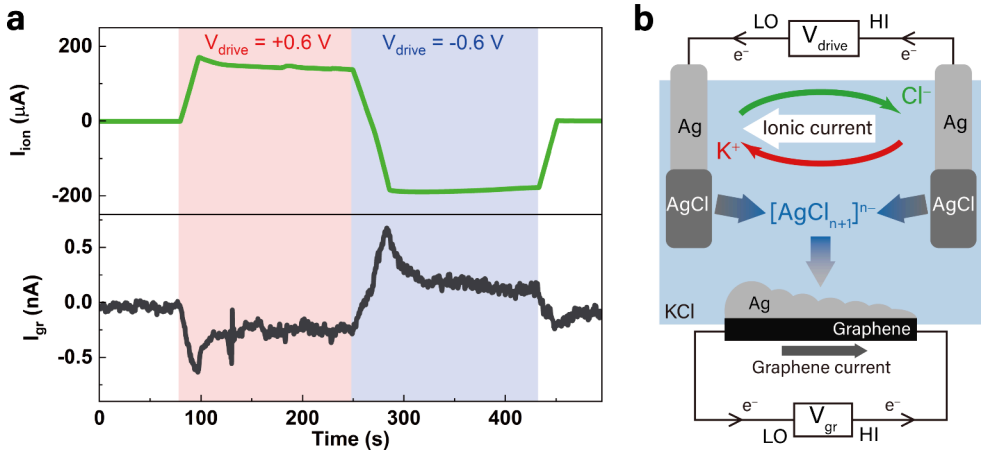

Figure 3. Electron current in graphene induced by silver electrodeposition. (a) Ionic current, I_{ion} (upper panel), generated between two Ag/AgCl electrodes with ±0.6 V driving voltage and a drag-like electronic current, I_{gr} (lower panel), induced in graphene. Regions colored in red and blue mark the driving voltage with opposite polarity. (b) Illustration of the current generation in graphene via electrodeposition of silver in our system. V_{drive} and V_{gr} are the drive voltage of the ion flow in the KCl solution and the voltage induced in graphene, respectively. The electrochemical reactions on two Ag/AgCl electrodes are AgCl(s) + e^- → Ag(s) + Cl^-(aq) and Ag(s) + Cl^-(aq) → AgCl(s) + e^-. The electrochemistry in the system can generate a graphene current with a reversed sign to the ionic current based on the electrodeposition of silver (not Coulomb drag). Arrows in green and red indicate the flow of Cl^- and K^+ ions. Arrows in gray/blue represent the formation and deposition of $[AgCl_{n+1}]^{n-}$.

reflect the silver distribution across the graphene sample after electrodeposition. It reveals that, unlike the uniform silver layer deposited on gold, the silver deposited on graphene aggregates into discrete small islands, consistent with the SEM images in Figure 1c. Our observations demonstrate the extent to which an Ag/AgCl electrode can contaminate an experimental system by introducing undesired silver-containing compounds to the solution and surfaces.

The electrodeposition of silver on graphene requires the dissolution of silver ions into the solution. To understand the excessive dissolution of AgCl in our system, we note that the common ion effect assumes that AgCl dissolves only to its constituent ions Ag^+ and Cl^- with an equilibrium of $K_{sp} = [Ag^+][Cl^-]$, where $K_{sp} = 1.8 \times 10^{-10}$ is the solubility product of AgCl at 25 °C[20] and square brackets represent the concentration in mol/L. Using this formula, Ag^+ introduced by AgCl dissolution is approximately 1.8×10^{-10} M in 1 M KCl solution, which can be safely disregarded in most systems. However, the dissolution of AgCl in Cl^--rich solutions that exceeds what is expected from the common ion effect has been known in the study of AgCl electrode degradation.[29,30] Instead of forming Ag^+ and Cl^- directly, AgCl forms $[AgCl_{n+1}]^{n-}$ complexes in the presence of Cl^-, increasing its solubility. This complex formation process is more pronounced in solutions with higher Cl^- concentrations. In a 3 M KCl solution, the solubility of AgCl is reported to reach approximately 2.4×10^{-3} M[31] at room temperature, 7 orders of magnitude higher than the prediction of the common ion effect alone.

We also conducted cyclic voltammetry (CV) to investigate the electrodeposition of silver on graphene using a three-electrode electrochemical cell, measured in 1 M KCl solution at a scan rate of 200 mV/min, as shown in Figure 2a. In this setup, a large, millimeter-sized CVD graphene served as the working electrode (see Figure S3a for the optical image of graphene after measurements). A patterned PDMS film was applied to protect the gold contacts from the electrolyte, ensuring that electrochemical reactions occurred exclusively on graphene. The exposed graphene area was approximately 6 mm^2. The reference electrode was an Ag/AgCl wire immersed in an isolated 3.4 M KCl solution, connected to the rest of the system through a leak-free junction manufactured by Innovative Instruments, Inc. This specialized junction prevents the passage of ions, effectively eliminating cross-contamination. A Keithley 2614 source meter was used to apply a voltage between graphene and the exposed Ag/AgCl counter electrode, and the potential difference between graphene and the reference electrode was monitored using a Keithley 2182A nanovoltmeter. This setup not only allows us to monitor the electrochemical process but also allows for the simultaneous gating of graphene. To evaluate the gate effect, a drain current of 100 nA at 30 Hz was applied, and the changes in graphene resistance were measured using an SR860 lock-in amplifier.

Figure 2b represents the cyclic voltammogram of the electrodeposition processes. The voltammogram shows one reduction peak and one oxidation peak, corresponding to the redox reaction of silver. These features indicate reaction dynamics similar to those previously reported for silver electrodeposition on HOPG,[32] ITO-coated glass,[33] and platinum[34] using $AgNO_3$ solutions. In our system, the absence of NO_3^- means that silver can only be oxidized to AgCl, a compound of low solubility compared to $AgNO_3$. Since silver ions in the solution originate primarily from the dissolution of the exposed Ag/AgCl electrode, any silver lost in the solution due to electrodeposition is rapidly replenished by the continuous dissolution of the Ag/AgCl electrode in the KCl solution. During this process, a sheer increase in the cathodic current is observed at negative potentials below −0.3 V (marked as the shaded yellow region). This can be partially attributed to the electrodeposition current. However, the reduction of oxygen from the dissolved air in an aqueous solution on the graphene surface could also contribute largely to this increase, as previously reported.[35] This reaction effectively enlarges the existing defects in graphene, aligning well with our observations, as CVD graphene samples consistently lose their integrity after prolonged CV scans (Figure S3a). The applied potential not only drives the electrochemical reaction but also gates graphene through the electrical double layer. This gating effect is demonstrated in

https://doi.org/10.1021/acs.nanolett.5c01929
Nano Lett. 2025, 25, 9427−9432

Figure 2c, where the graphene resistance reaches a maximum at around 0.11 V, corresponding to the charge neutrality point of graphene. However, noticeable shoulders in the curves suggest strong inhomogeneity of the sample, as a result of the possible damage to graphene during continuous measurements. In the context of gating graphene, the current in Figure 2b can also be interpreted as the gate "leakage current", which should ideally be zero. Therefore, in liquid gating systems, it is recommended to employ a lock-in technique to minimize the interference of the DC leakage current with the drain current measurements.

We have shown that in a system with concentrated Cl^-, the dissolution of AgCl rapidly introduces $[AgCl_{n+1}]^{n-}$ complexes into the solution, making silver contamination a significant issue. Silver contaminants may further interfere with the intended measurements, which, if overlooked, may lead to misinterpretation of experimental results. To highlight its impact, we report the silver contamination issues encountered during our investigation of "ionic Coulomb drag". This is one of the phenomena where ionic flow across the graphene surface has been reported to generate electricity.[36−43] Despite ongoing efforts to unravel the underlying physics, considerable debate remains regarding the electricity geneartion mechanism. Ionic Coulomb drag refers to the momentum transfer from moving ions in a solution to electrons in a nearby solid, such as graphene, through Coulomb interactions. Several recent studies[18,44,45] have reported the observation of this effect in microfluidic systems, underlining its potential for energy harvesting and sensing applications.

Different experimental configurations were used to investigate this phenomenon. Figure 3b shows one measurement configuration. In this setup, a millimeter-sized CVD graphene was positioned between two Ag/AgCl electrodes in a liquid channel filled with 1 M KCl solution. An ionic flow was generated by applying a voltage bias across a pair of Ag/AgCl electrodes. At each electrode, the $Ag(s) + Cl^- \leftrightarrow AgCl(s) + e^-$ reaction locally generates or consumes silver ions (depending on bias polarity), causing Cl^- to migrate between two electrodes, accompanied by a corresponding K^+ flow.[46,47] In our experiments, ± 0.6 V voltage was applied between two Ag/AgCl electrodes using one channel of a Keithley 2614 source meter, and the current generated in graphene was measured using the second channel of the source meter.

This measurement setup closely followed the methodology of an earlier study[18], and indeed, we observed similar signals. The upper panel of Figure 3a shows the ionic current generated in the solution, while the lower panel shows the electronic current induced in graphene in response to the ionic current. With a μA-level ionic current, a sign-reversed nA-level electronic current is observed in graphene. The observed characteristics, particularly the sign-reversed electronic current, are consistent with the previously proposed "ionic Coulomb drag" explanation. However, after repeating the same experiments on dozens of similar graphene devices, we observed significant variations in the measured results, both in magnitude and sign-reversal behaviour. In fact, in half of the tested devices, the measured electronic current became sign-aligned with the ionic current (Figure S6). Such randomness makes the "ionic Coulomb drag" untenable and an alternative interpretation is needed.

In the experiment, although the Ag/AgCl electrodes and graphene are electrically isolated, they remain coupled through the electrodeposition process, allowing ions and electrons to interchange. Importantly, the source meter connected to graphene can act as an electron source or sink even without applying a voltage, supplying electrons necessary for silver electrodeposition. Hence, we propose that the electronic current detected in graphene is solely due to silver deposition rather than Coulomb drag! See Figure S3b for the optical micrograph of the graphene device after measurements, with profound silver-containing particles deposited on graphene. Figure 3b illustrates this mechanism: AgCl dissolves in the KCl solution, forming silver complexes $[AgCl_{n+1}]^{n-}$. Under an applied voltage between the Ag/AgCl electrodes, generating an electronic current. If the deposition were perfectly even (which is unlikely), the currents would cancel out, and no net current would appear. In reality, the deposition is always uneven, so we detect a current. The strength and direction of this current depend on how much silver is deposited and where it starts. Variations in current magnitude and sign arise from differences in deposition extent and location on graphene, explaining the observed inconsistencies across multiple devices (cf. 3a and Figure S6 in the Supporting Information). Thus, the generation of electronic current in graphene depends exclusively on silver redox reactions, independent of direct ionic interactions with graphene.

More generally, silver contamination also impacts other experimental systems in nanoscience. Take graphene in solution as an example. Ag/AgCl electrode is often used as a liquid gate electrode for graphene transistors for sensing purposes. For graphene sensors which operate based on the doping of graphene, the unintended silver deposition may serve as additional dopants, compromising their sensitivity and detection accuracy. Fortunately, in these cases, the issue can be avoided by replacing the Ag/AgCl electrode with less soluble materials like platinum (Pt), or by applying only positive potentials on the graphene. In practice, Ag/AgCl electrode dissolution may still be considered negligible in systems such as ionic transport through nanopores and nanochannels, where the concentration of silver ions remains significantly lower than that of the primary ionic species. However, in systems where Ag/AgCl electrode pair is used to drive ionic current, such as the "ionic Coulomb drag" experiment, it is challenging to fully remove silver contamination. An alternative method for driving the ionic flow may be required, for example, osmotic flow driven by a concentration gradient. Another way is to measure only the open-circuit voltage across graphene throughout the experiment using a voltmeter with sufficiently high input resistance, as this can effectively reduce the electrochemical reactions.

In summary, we demonstrate that the dissolution of AgCl in Cl^--rich aqueous systems can introduce serious contamination, which, if overlooked, could lead to misinterpretation of experimental results in such systems. Ag/AgCl electrodes, despite their frequent usage in nanoscience, could cause significant complications to the system. Care should be taken when applying Ag/AgCl electrodes in ion-sensitive environments, especially with high Cl^- concentrations. Ag/AgCl electrodes should be isolated appropriately using low-leak or leak-free junctions, even when used only as reference electrodes.

https://doi.org/10.1021/acs.nanolett.5c01929
Nano Lett. 2025, 25, 9427−9432

■ ASSOCIATED CONTENT

Supporting Information

The Supporting Information is available free of charge at https://pubs.acs.org/doi/10.1021/acs.nanolett.5c01929.

Experimental methods of SEM, EDX, Raman spectroscopy, and electronic measurement. Fabrication methods for graphene electrodes and Ag/AgCl electrodes. EDX mapping for silver-deposited graphene. Raman spectra of pure Ag and pure AgCl. Additional optical micrographs of silver-deposited CVD graphene and mechanically exfoliated graphene. Summary of other devices measured in the investigation of "ionic Coulomb drag". (PDF)

■ AUTHOR INFORMATION

Corresponding Authors

Chuhongxu Chen − *Department of Physics and Astronomy, University of Manchester, Manchester M13 9PL, U.K.*; Email: chuhongxu.chen@postgrad.manchester.ac.uk

Artem Mishchenko − *Department of Physics and Astronomy, University of Manchester, Manchester M13 9PL, U.K.; National Graphene Institute, University of Manchester, Manchester M13 9PL, U.K.*; orcid.org/0000-0002-0427-5664; Email: artem.mishchenko@manchester.ac.uk

Qian Yang − *Department of Physics and Astronomy, University of Manchester, Manchester M13 9PL, U.K.; National Graphene Institute, University of Manchester, Manchester M13 9PL, U.K.*; orcid.org/0000-0002-6203-7867; Email: qian.yang@manchester.ac.uk

Authors

Ziwei Wang − *Department of Physics and Astronomy, University of Manchester, Manchester M13 9PL, U.K.*

Guilin Chen − *Department of Physics and Astronomy, University of Manchester, Manchester M13 9PL, U.K.*

Zhijia Zhang − *Department of Physics and Astronomy, University of Manchester, Manchester M13 9PL, U.K.*

Zakhar Bedran − *Department of Physics and Astronomy, University of Manchester, Manchester M13 9PL, U.K.*

Stephen Tipper − *Department of Physics and Astronomy, University of Manchester, Manchester M13 9PL, U.K.*

Pablo Diaz-Núñez − *Department of Physics and Astronomy, University of Manchester, Manchester M13 9PL, U.K.*

Ivan Timokhin − *Department of Physics and Astronomy, University of Manchester, Manchester M13 9PL, U.K.*

Complete contact information is available at: https://pubs.acs.org/10.1021/acs.nanolett.5c01929

Notes

The authors declare no competing financial interest.

■ ACKNOWLEDGMENTS

The authors thank Prof Irina Grigorieva for very useful discussion regarding this work. This research is supported by the Royal Society University Research Fellowship URF \R1\221096 and UK Research and Innovation Grant [EP/X017575/1]. Artem Mishchenko acknowledges the funding from the European Research Council (ERC) under the European Union's Horizon 2020 research and innovation program (Grant Agreement No. 865590) and the Research Council UK [BB/X003736/1].

■ REFERENCES

(1) Brown, A. S. A Type of Silver Chloride Electrode Suitable for Use in Dilute Solutions. *J. Am. Chem. Soc.* **1934**, *56*, 646−647.

(2) Kireev, D.; Brambach, M.; Seyock, S.; Maybeck, V.; Fu, W.; Wolfrum, B.; Offenhäusser, A. Graphene transistors for interfacing with cells: towards a deeper understanding of liquid gating and sensitivity. *Sci. Rep.* **2017**, *7*, 6658−12.

(3) Zhan, H.; Cervenka, J.; Prawer, S.; Garrett, D. J. Molecular detection by liquid gated Hall effect measurements of graphene. *Nanoscale* **2018**, *10*, 930−935.

(4) He, R. X.; Lin, P.; Liu, Z. K.; Zhu, H. W.; Zhao, X. Z.; Chan, H. L. W.; Yan, F. Solution-Gated Graphene Field Effect Transistors Integrated in Microfluidic Systems and Used for Flow Velocity Detection. *Nano Lett.* **2012**, *12*, 1404−1409.

(5) Traversi, F.; Raillon, C.; Benameur, S. M.; Liu, K.; Khlybov, S.; Tosun, M.; Krasnozhon, D.; Kis, A.; Radenovic, A. Detecting the translocation of DNA through a nanopore using graphene nanoribbons. *Nature Nanotechnol.* **2013**, *8*, 939−945.

(6) Agrawal, K. V.; Drahushuk, L. W.; Strano, M. S. Observation and analysis of the Coulter effect through carbon nanotube and graphene nanopores. *Philosophical transactions of the Royal Society of London. Series A: Mathematical, physical, and engineering sciences* **2016**, *374*, 20150357.

(7) Garaj, S.; Liu, S.; Golovchenko, J. A.; Branton, D. Molecule-hugging graphene nanopores. *Proceedings of the National Academy of Sciences - PNAS* **2013**, *110*, 12192−12196.

(8) Jiang, X.; Zhao, C.; Noh, Y.; Xu, Y.; Chen, Y.; Chen, F.; Ma, L.; Ren, W.; Aluru, N. R.; Feng, J. Nonlinear electrohydrodynamic ion transport in graphene nanopores. *Science advances* **2022**, *8*, No. eabj2510.

(9) Rollings, R. C.; Kuan, A. T.; Golovchenko, J. A. Ion selectivity of graphene nanopores. *Nat. Commun.* **2016**, *7*, 11408−11408.

(10) Jain, T.; Rasera, B. C.; Guerrero, R. J. S.; Boutilier, M. S. H.; O'Hern, S. C.; Idrobo, J.-C.; Karnik, R. Heterogeneous sub-continuum ionic transport in statistically isolated graphene nanopores. *Nature Nanotechnol.* **2015**, *10*, 1053−1057.

(11) Feng, J.; Liu, K.; Bulushev, R. D.; Khlybov, S.; Dumcenco, D.; Kis, A.; Radenovic, A. Identification of single nucleotides in MoS2 nanopores. *Nature Nanotechnol.* **2015**, *10*, 1070−1076.

(12) Su, S.; Zhang, Y.; Peng, S.; Guo, L.; Liu, Y.; Fu, E.; Yao, H.; Du, J.; Du, G.; Xue, J. Multifunctional graphene heterogeneous nanochannel with voltage-tunable ion selectivity. *Nat. Commun.* **2022**, *13*, 4894−4894.

(13) Zhang, P.; Xia, M.; Zhuge, F.; Zhou, Y.; Wang, Z.; Dong, B.; Fu, Y.; Yang, K.; Li, Y.; He, Y.; Scheicher, R. H.; Miao, X. S. Nanochannel-Based Transport in an Interfacial Memristor Can Emulate the Analog Weight Modulation of Synapses. *Nano Lett.* **2019**, *19*, 4279−4286.

(14) Golovchenko, J. A.; Kong, J.; Reina, A.; Hubbard, W.; Garaj, S.; Branton, D. Graphene as a subnanometre trans-electrode membrane. *Nature (London)* **2010**, *467*, 190−193.

(15) Schneider, G. F.; Kowalczyk, S. W.; Calado, V. E.; Pandraud, G.; Zandbergen, H. W.; Vandersypen, L. M. K.; Dekker, C. DNA Translocation through Graphene Nanopores. *Nano Lett.* **2010**, *10*, 3163−3167.

(16) Freedman, K. J.; Ahn, C. W.; Kim, M. J. Detection of Long and Short DNA Using Nanopores with Graphitic Polyhedral Edges. *ACS Nano* **2013**, *7*, 5008−5016.

(17) Bonaccini Calia, A.; et al. Full-bandwidth electrophysiology of seizures and epileptiform activity enabled by flexible graphene microtransistor depth neural probes. *Nature Nanotechnol.* **2022**, *17*, 301−309.

(18) Chen, F.; Zhao, Y.; Saxena, A.; Zhao, C.; Niu, M.; Aluru, N. R.; Feng, J. Inducing Electric Current in Graphene Using Ionic Flow. *Nano Lett.* **2023**, *23*, 4464−4470.

(19) Xiong, M.; Song, K.; Leburton, J.-P. Ionic coulomb drag in nanofluidic semiconductor channels for energy harvest. *Nano energy* **2023**, *117*, 108860.

(20) Rumble, J. R. *CRC handbook of chemistry and physics*, ninety-ninth ed.; CRC Press: Boca Raton, 2018.
(21) Levard, C.; Hotze, E. M.; Lowry, G. V.; Brown, G. E. Environmental Transformations of Silver Nanoparticles: Impact on Stability and Toxicity. *Environ. Sci. Technol.* **2012**, *46*, 6900−6914.
(22) Cortijo-Campos, S.; Ramírez-Jiménez, R.; Climent-Pascual, E.; Aguilar-Pujol, M.; Jiménez-Villacorta, F.; Martínez, L.; Jiménez-Riobóo, R.; Prieto, C.; de Andrés, A. Raman amplification in the ultra-small limit of Ag nanoparticles on SiO2 and graphene: Size and inter-particle distance effects. *Materials & Design* **2020**, *192*, 108702.
(23) Li, Z.; Huang, J.; Zhong, J.; Li, J. Preparation of AgCl with enhanced photocatalytic activity using ionic liquid as chlorine source. *Applied physics. A, Materials science & processing* **2020**, *126*, 554.
(24) Otto, A. Raman scattering from adsorbates on silver. *Surface science* **1980**, *92*, 145−152.
(25) Atkinson, G.; Guzonas, D.; Irish, D. Raman spectral studies at the silver surface of the Ag|KCl, pyridine electrode. *Chemical physics letters* **1980**, *75*, 557−560.
(26) Martina, I.; Wiesinger, R.; Jembrih-Simbuerger, D.; Schreiner, M. Micro-Raman characterisation of silver corrosion products. *e-Preservation Science* **2012**, *9*, 1−8.
(27) Nagiri, R.; Kumar, K.; Aryasomayajula, S. Silver oxide (AgO) thin films for Surface Enhanced Raman Scattering (SERS) studies. *AIP Conf. Proc.* **2010**, *1267*, 1005−1006.
(28) Caro, C.; Zaderenko, A. P.; Gámez, F.; Krafft, C. Preparation of Surface-Enhanced Raman Scattering Substrates Based on Immobilized Silver-Capped Nanoparticles. *Journal of spectroscopy (Hindawi)* **2018**, *2018*, 1−9.
(29) Suzuki, H.; Hiratsuka, A.; Sasaki, S.; Karube, I. Problems associated with the thin-film Ag/AgCl reference electrode and a novel structure with improved durability. *Sensors and actuators. B, Chemical* **1998**, *46*, 104−113.
(30) Roger, I.; Symes, M. D. Silver Leakage from Ag/AgCl Reference Electrodes as a Potential Cause of Interference in the Electrocatalytic Hydrogen Evolution Reaction. *ACS Appl. Mater. Interfaces* **2017**, *9*, 472−478.
(31) Ito, S.; Hachiya, H.; Baba, K.; Asano, Y.; Wada, H. Improvement of the silver/silver chloride reference electrode and its application to pH measurement. *Talanta (Oxford)* **1995**, *42*, 1685−1690.
(32) Lai, S. C. S.; Lazenby, R. A.; Kirkman, P. M.; Unwin, P. R. Nucleation, aggregative growth and detachment of metal nanoparticles during electrodeposition at electrode surfaces. *Chemical science (Cambridge)* **2015**, *6*, 1126−1138.
(33) Hasan, G. G.; Khelef, A.; Chaabia, N.; Tedjani, M. L.; Althamthami, M. Electrochemical deposition of Ag nanoparticles on ITO-coated glass: effect of different cyclic voltammetry scan rates on Ag deposition. *Ferroelectrics* **2023**, *602*, 121−134.
(34) Huan, T. N.; Kim, S.; Van Tuong, P.; Chung, H. Au−Ag bimetallic nanodendrite synthesized via simultaneous co-electrodeposition and its application as a SERS substrate. *RSC Adv.* **2014**, *4*, 3929−3933.
(35) Svetlova, A.; Kireev, D.; Beltramo, G.; Mayer, D.; Offenhäusser, A. Origins of Leakage Currents on Electrolyte-Gated Graphene Field-Effect Transistors. *ACS applied electronic materials* **2021**, *3*, 5355−5364.
(36) Ghosh, S.; Sood, A. K.; Kumar, N. Carbon Nanotube Flow Sensors. *Science (American Association for the Advancement of Science)* **2003**, *299*, 1042−1044.
(37) Dhiman, P.; Yavari, F.; Mi, X.; Gullapalli, H.; Shi, Y.; Ajayan, P. M.; Koratkar, N. Harvesting Energy from Water Flow over Graphene. *Nano Lett.* **2011**, *11*, 3123−3127.
(38) Yin, J.; Zhang, Z.; Li, X.; Zhou, J.; Guo, W. Harvesting Energy from Water Flow over Graphene? *Nano Lett.* **2012**, *12*, 1736−1741.
(39) Ho Lee, S.; Jung, Y.; Kim, S.; Han, C.-S. Flow-induced voltage generation in non-ionic liquids over monolayer graphene. *Applied physics letters* **2013**, *102*, 063116.
(40) Kuriya, K.; Ochiai, K.; Kalita, G.; Tanemura, M.; Komiya, A.; Kikugawa, G.; Ohara, T.; Yamashita, I.; Ohuchi, F. S.; Meyyappan, M.; Samukawa, S.; Washio, K.; Okada, T. Output density quantification of electricity generation by flowing deionized water on graphene. *Applied physics letters* **2020**, *117*, 123905.
(41) Lizée, M.; Marcotte, A.; Coquinot, B.; Kavokine, N.; Sobnath, K.; Barraud, C.; Bhardwaj, A.; Radha, B.; Niguès, A.; Bocquet, L.; Siria, A. Strong Electronic Winds Blowing under Liquid Flows on Carbon Surfaces. *Physical review* **2023**, *13*, 011020.
(42) Kaźmierczak, P.; Binder, J.; Boryczko, K.; Ciuk, T.; Strupiński, W.; Stępniewski, R.; Wysmołek, A. Direction-sensitive graphene flow sensor. *Applied Physics Letters* **2023**, *123*, 263507.
(43) Takeda, H.; Iwamoto, N.; Honda, M.; Tanemura, M.; Yamashita, I.; Komiya, A.; Okada, T. Investigating the correlation between flow dynamics and flow-induced voltage generation. *Applied Physics Letters* **2024**, *125*, 184101.
(44) Jiang, Y.; Liu, W.; Wang, T.; Wu, Y.; Mei, T.; Wang, L.; Xu, G.; Wang, Y.; Liu, N.; Xiao, K. A nanofluidic chemoelectrical generator with enhanced energy harvesting by ion-electron Coulomb drag. *Nat. Commun.* **2024**, *15*, 8582−8.
(45) Rabinowitz, J.; Cohen, C.; Shepard, K. L. An Electrically Actuated, Carbon-Nanotube-Based Biomimetic Ion Pump. *Nano Lett.* **2020**, *20*, 1148−1153.
(46) Cho, K. R.; Kim, M.; Kim, B.; Shin, G.; Lee, S.; Kim, W. Investigation of the AgCl Formation Mechanism on the Ag Wire Surface for the Fabrication of a Marine Low-Frequency-Electric-Field-Detection Ag/AgCl Sensor Electrode. *ACS omega* **2022**, *7*, 25110−25121.
(47) Katan, T.; Szpak, S.; Bennion, D. N. Silver/Silver Chloride Electrodes: Surface Morphology on Charging and Discharging. *J. Electrochem. Soc.* **1974**, *121*, 757−764.

https://doi.org/10.1021/acs.nanolett.5c01929
Nano Lett. 2025, 25, 9427−9432